

## 6. DATA REPORT: DIATOM FLORA OF THE NORTHERN CALIFORNIA MARGIN SINCE 3 MA<sup>1</sup>

Akihiro Ikeda<sup>2</sup> and Itaru Koizumi<sup>2</sup>

### INTRODUCTION

The Pliocene and Pleistocene periods are known for the onset and consequent amplification of glacial–interglacial cycles. The California margin, situated in the mid-latitudes of the northern Pacific Ocean, is expected to be one of the most interesting regions for Pliocene to Pleistocene paleoceanography because this area occupies a unique position in the ocean–atmosphere system over the region. In this study, we investigated paleoceanographic history, using fossil diatoms, since the Brunhes/Matuyama (B/M) paleomagnetic boundary in which glacial and interglacial periods began to alternate in 100-yr cycles. In Hole 1018A, to a depth corresponding to the beginning of Northern Hemisphere glaciation (late Pliocene), we investigated the responses of the ocean–atmosphere system to stepwise cooling in the California margin. Although the work is still continuing, this data report shows that fossil diatoms of Pliocene and Pleistocene sediments significantly changed both in quality and quantity and implies a possible relationship to global climatic changes.

### OCEANIC AND ATMOSPHERIC OVERVIEW

The studied sites (Sites 1018, 1020, and 1021) are situated at ~40°N, where the California Current flows to the south (Fig. 1). The California Current, which is formed at the Polar Front as the edge of the subtropical gyre, brings relatively cold water to this region.

This region is affected by Pacific high pressure all through the year; especially in summer, this high pressure creates strong north-west winds, which cause an enhancement of Ekman upwelling in the northern coastal region. In winter, however, wind stress is weakened because the Aleutian low-pressure cell gains power; subsequently, coastal upwelling is also weakened and moves southward.

### MATERIALS AND PROCEDURES

Site 1018 (36°59'N, 123°17'W; water depth, 2477 m) is coastal and shallow, located on the sediment drift at the flank of the Guide Seamount, and the sedimentation rate is relatively high compared to those of the other two sites (157 m/m.y. on average).

Site 1020 (41°00'N, 126°26'W; water depth, 3038.4 m) is situated on the east flank of Gorda Basin and is ~170 km west from shore. This is a paleoceanographically well-defined site; the oxygen isotope record (A. Mix, pers. comm., 1998) and the calcium carbonate and biogenic opal records (Kuroda et al., Chap. 14, this volume) of the late Pleistocene have been already obtained.

Site 1021 (39°05'N, 127°47'W; water depth, 4211.5 m) is located on the Outer Delgada Fan, ~360 km from shore. The extremely low sedimentation rate (779 m/m.y.) and the siliciclastic clay sediments seem to reflect very low biogenic production in the sea surface above this drill site.

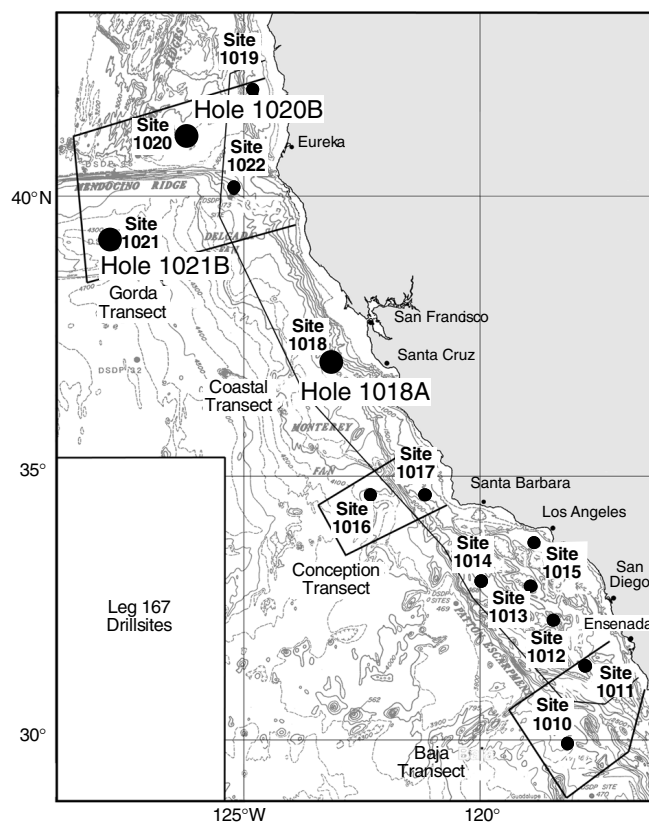


Figure 1. Location map for Leg 167 drill sites along the California margin of North America (Shipboard Scientific Party, 1997).

Samples for the C1n (Brunhes) Subchron were taken at roughly 70-cm intervals: time intervals for Sites 1018, 1020, and 1021 correspond to sampling intervals of ~5, ~8, and ~21 ka, respectively. Samples representing the early Pleistocene and the late Pliocene were taken at roughly 340-cm intervals down to Core 39X for Hole 1018A.

A set of strewn slides was prepared following the modified procedures used by Koizumi (1992) and Ikeda et al. (2000). After drying in an oven at 50°C for 24 hr, 0.1 g ( $\pm 5\%$ ) of the sample was dissolved in 10 mL of hydrogen peroxide solution (15% strength) in a 100-mL beaker and boiled for several minutes. After filling with distilled water, the beaker was left to stand for 5 hr. Then the supernatant was poured off, and distilled water was poured in again. This decanting process was repeated four times to dilute acidity in the suspension. The residue was finally diluted with 100 mL of distilled water and homogenized for several seconds in an ultrasonic bath. Using a micropipette, 0.5 mL of this solution was spread on a square cover glass (18 × 18 mm) and dried on a hot plate at 50°C. The prepared cover glass was mounted on a glass slide using Pleurax.

All diatoms were identified and counted under a light microscope with magnification of 600× until the total number exceeded 200 (resting spores of *Chaetoceros* spp. not included). The counting was accomplished by observing up to six traverses spanning the entire width

<sup>1</sup>Lyle, M., Koizumi, I., Richter, C., and Moore, T.C., Jr. (Eds.), 2000. *Proc. ODP, Sci. Results*, 167: College Station TX (Ocean Drilling Program).

<sup>2</sup>Division of Earth and Planetary Sciences, Graduate School of Science, Hokkaido University, Sapporo, 060-0818, Japan. Correspondence author: itaru@ep.sci.hokudai.ac.jp

of the cover glass. The total number did not reach 200 specimens when diatoms were sparse. Because the weight of sediment on a cover glass is measurable, the abundance of diatom valves (number per gram) was obtained by using the numbers of transects and the total amount of diatom valves. The results are presented in Tables 1, 2, and 4 (on back-pocket foldout, this volume) and in Table 3.

Diatom abundance fluctuates significantly at Sites 1018 and 1020, whereas diatoms are very scarce in the section studied at Site 1021. In general, when the total number did not reach 200 specimens, representative diatom assemblages could not be obtained even by relative abundance (percentage of total diatom valves) because the value contains a statistically serious error. Therefore, all taxonomic abundances were indicated by absolute values (number of diatom valves per gram of sediment).

Judging conditions of preservation depended on the extent of dissolution, fragmentation, and overgrowth of diatom valves through observation with a light microscope.

## PALEOCEANOGRAPHY SINCE THE B/M BOUNDARY

### Diatom Abundance and Preservation

The numbers of diatom valves fluctuate significantly with depth, between ten thousand and several tens of millions of valves per gram of sediment (Fig. 2). When compared to  $\delta^{18}\text{O}$  stages for the upper 24 meters below seafloor (mbsf) defined by Andreasen et al., Chap. 8 (this volume), it is clear that diatom valves decrease at the end of glacial periods. This trend is also observed at depths above 34 mbsf at Site 1020. At 34 mbsf, diatom valves are very few and then increase gradually until 10 mbsf (Fig. 3). This probably resulted from improved opal preservation. The B/M boundary was not identified at Site 1018, but the patterns of fluctuation of diatom abundance—which were very similar at Sites 1018 and 1020—were compared, and the depth of 123.5 mbsf was assumed for that event. Diatom abundance at Site 1021 is extremely low, less than ten thousand valves per gram of sediment in the upper 5 m, and very rarely identified at the depths below that. Preservation is very poor (Fig. 4).

### Changes in Diatom Assemblages

At Site 1020 (Fig. 5), the cold-water species *Neodenticula seminae* dominates in the lower part (84.7–50.0 meters composite depth [mcd]), although there is an interval of low concentration of diatoms between 75.3 and 64.7 mcd. A strong peak in abundance of the freshwater group, such as *Aulacoseira* spp., *Flagilaria* spp., and *Stephanodiscus* spp., appears at 41.1 mcd. In the upper stages, there is a relatively high concentration and successively increasing productivity of diatoms. The top of the sample, which indicates warm conditions, corresponds to the Holocene.

After “the mid-Brunhes climatic event” around 400 ka (Jansen et al., 1986), conditions of the sea surface changed from pelagic to more coastal and productive. As shown in Figure 5, the subsequent changes in abundance of the freshwater group are in short cycles (~5 m). These may correspond to a cycle shorter than the typical glacial–interglacial cycle (such as obliquity or climatic precession) and imply that the freshwater group is transported by seasonal winds and/or enhanced precipitation because both are thought to fluctuate in precessional cycles.

At Site 1018 (Fig. 6), on the other hand, dominance of freshwater species is observed during 127–115, 95–85, and 65–52 mcd; diatoms are generally scarce at the corresponding depths of Site 1020. A short cycle cannot be observed in the fluctuating abundance of the freshwater group, but it is interesting that compared to total diatom abundance, the freshwater group increases during periods of low concentration of diatom valves (the glacial periods). If the fluctuation of diatom abun-

dance corresponds to glacial–interglacial cycles in the entire C1n Subchron, this correlation with glacial cycles apparently resulted from falling sea level and increasing terrigenous inflow.

## STRATIGRAPHIC DISTRIBUTION OF MAJOR SPECIES BETWEEN 3 AND 0.8 MA

Since 3 Ma at Site 1018, diatom valves decrease during glacial periods, and the fluctuation of diatom abundance decreases during the interval between 3 and 0.8 Ma (Fig. 7). The cold-water species *Neodenticula* spp. (*N. kamtschatica*, *N. koizumii*, and *N. seminae*) are predominant. Four diatom datum levels are recognized at Site 1018 as follows: last occurrence (LO) of *N. kamtschatica* (2.6–2.7 Ma) is recognized between Samples 167-1018A-38X-4, 143 cm, and 38X-6, 140 cm (between 355.32 and 358.29 mbsf); LO of *N. koizumii* (2.0 Ma) between Samples 167-1018A-25X-6, 136 cm, and 26X-2, 142 cm (between 233.05 and 236.71 mbsf); first occurrence (FO) of *Rhizosolenia matuyamai* (1.18 Ma) between Samples 167-1018A-18X-7, 141 cm, and 19X-2, 141 cm (between 166.12 and 169.40 mbsf); and LO of *R. matuyamai* (1.02 Ma) between Samples 167-1018A-17X-6, 141 cm, and 18X-3, 141 cm (between 156.2 and 160.12 mbsf). The age assignments of Baldauf and Iwai (1995) and Yanagisawa and Akiba (1998) were recalibrated to the geomagnetic time scale of Cande and Kent (1995).

The floral succession of the last 3 m.y. is summarized in four stages.

Stage 1: Oceanic–environmental stage (387.5–260 mcd): *Thalassionema nitzschioides*, *N. koizumii*, and *Stephanopyxis* spp. are predominant, and *Azpeitia nodulifera*, *Thalassiosira oestrupii*, and *Coscinodiscus marginatus* are dominant (Table 4).

Stage 2: High-productivity stage (260–206 mcd): *T. nitzschioides* and *N. seminae* are predominant.

Stage 3: Low-productivity stage (206–138 mcd): diatoms are scarce, and *Stephanopyxis turris* and *N. seminae* are present.

Stage 4: High-productivity stage (138–0 mcd): *T. nitzschioides* and *N. seminae* are predominant.

## SUMMARY

1. Diatom productivity can be estimated roughly by means of abundance and lithology: at the offshore site (Site 1021), it is poorest probably because of its location in a subtropical gyre; at the coastal site (Site 1018), it is richest.

2. Diatoms are abundant during interglacial periods and are rare during glacial periods.

3. Marine conditions changed from oceanic to more coastal and productive ~400 ka.

4. The fluctuation pattern of freshwater diatoms at Site 1020 is different from the pattern at Site 1018; patterns in the former suggest shorter cycles such as precession or obliquity, and those in the latter suggest eccentricity-related 100-k.y. cycles. There seem to be several causes for increased transportation of freshwater diatoms.

5. Four diatom datum levels (LO of *N. kamtschatica*, LO of *N. koizumii*, and FO and LO of *R. matuyamai*) are recognized since 3.0 Ma at Site 1018.

## ACKNOWLEDGMENTS

We thank the co-chief, shipboard scientists, technicians, and crew of the *JOIDES Resolution* for their assistance and cooperation in obtaining the samples. We wish to express our gratitude to Dr. John Barron, U.S. Geological Survey, for reading the manuscript. Our thanks is also extended to Mr. M. Shiono, Hokkaido University, for his valuable advice on identification of diatoms.

Table 3. Distribution chart of diatom species at Site 1021.

Core, section, interval (cm)	Depth (mbsf)	Depth (mcd)	Preservation	Diatom valves (no./g)	<i>Chaetoceros</i> spp. resting spores	<i>Actinocyclus oculatus</i>	<i>Actinopychnus senarius</i>	<i>Aulacoseira</i> spp.	<i>Coscinodiscus radiatus</i>	<i>Delphineis surirella</i>	<i>Fragilaria</i> spp.	<i>Melosira</i> spp.	<i>Navicula</i> spp.	<i>Neodenticula seminatae</i>	<i>Paralia sulcata</i>	<i>Pinnularia</i> spp.	<i>Rhaphoneis amphiceros</i>	<i>Rhaphoneis paralis</i>	<i>Rhizosolenia styliformis</i>	<i>Rhoicosphaenia</i> spp.	<i>Stephanodiscus astrea</i>	<i>Stephanopyxis turris</i>	<i>Synedra</i> spp.	<i>Thalassiosira decipiens</i>	<i>Thalassiosira gravida</i>	<i>Thalassionema nitzschioideis</i>	<i>Thalassionema nitzschioideis</i> var. <i>parva</i>	<i>Thalassiothrix frauenfeldii</i>	<i>Thalassiothrix longissima</i>	Total counts	
167-1021B-																															
1H-1, 70-72	0.70	0.70	M	2.01E+05	6		2	1		1		1		2	1						1			1		6	2	1	1	20	
1H-1, 140-142	1.40	1.40	P	1.21E+05	1		4	1			1		1							1	1			1	1	2				12	
1H-2, 70-72	2.20	2.20	M	6.04E+04	1		3									2		1												6	
1H-2, 140-142	2.90	2.90	M	1.61E+05	3		3				1		1									3	1		3	3		1		16	
1H-3, 70-72	3.70	3.70	P	8.05E+04			3																			1	1			8	
1H-3, 140-142	4.40	4.40	M	2.01E+04											3											2				2	
1H-4, 70-72	5.20	5.20	—	0.00E+00	1																									0	
1H-4, 140-142	5.90	5.90	—	0.00E+00																										0	
1H-5, 70-72	6.70	6.70	—	0.00E+00																										0	
1H-5, 140-142	7.40	7.40	—	0.00E+00																										0	
2H-1, 70-72	8.70	9.88	—	0.00E+00																										0	
2H-1, 140-142	9.40	10.58	—	0.00E+00																										0	
2H-2, 70-72	10.20	11.38	—	0.00E+00																										0	
2H-2, 140-142	10.90	12.08	—	0.00E+00																										0	
2H-3, 56-58	11.70	12.88	—	0.00E+00																										0	
2H-3, 140-142	12.40	13.58	—	0.00E+00																										0	
2H-4, 70-72	13.20	14.38	—	0.00E+00																										0	
2H-4, 140-142	13.90	15.08	P	2.01E+04	1																					2				2	
2H-5, 70-72	14.70	15.88	P	0.00E+00																										0	
2H-5, 140-142	15.40	16.58	—	0.00E+00																										0	
2H-6, 70-72	16.20	17.38	—	0.00E+00																										0	
2H-6, 140-142	16.90	18.08	—	0.00E+00																										0	
2H-7, 66-68	17.66	18.84	P	1.01E+04	3												1													1	
3H-1, 70-72	18.20	20.14	P	1.01E+05				7						1												2				10	
3H-1, 140-142	18.90	20.84	P	1.01E+04																										1	
3H-2, 70-72	19.70	21.64	—	0.00E+00																										0	
3H-2, 140-142	20.40	22.34	P	2.01E+04			1																							2	
3H-3, 70-72	21.20	23.14	P	1.01E+04																							1				1
3H-3, 140-142	21.90	23.84	—	0.00E+00																										0	
3H-4, 70-72	22.70	24.64	P	2.01E+04	1			1						1																2	
3H-4, 140-142	23.40	25.34	P	1.01E+04																											1
3H-5, 70-72	24.20	26.14	—	0.00E+00																										0	
3H-5, 140-142	24.90	26.84	P	2.01E+04										1												1				2	
3H-6, 70-72	25.70	27.64	P	2.01E+04										2																2	

Note: M = moderate, P = poor, — = no diatoms.

This table also appears on the volume CD-ROM.

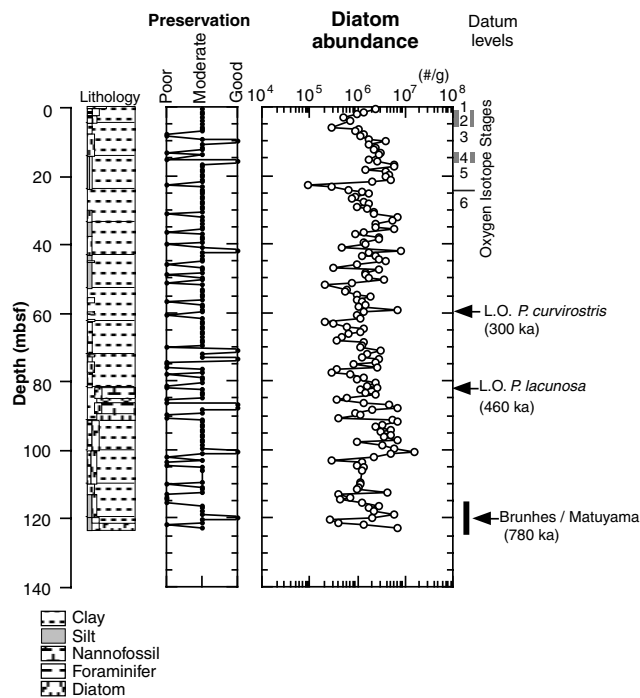


Figure 2. Stratigraphic variations in the abundance and preservation of diatom valves in Hole 1018A. Oxygen isotope stages were derived by Andreasen et al. (Chap. 8, this volume). LO (last occurrence) of *Proboscia curvirostris* was from Table 1 (this chapter), and LO of *Pseudoemiliania lacunosa* (calcareous nannofossil) was from Shipboard Scientific Party (1997).

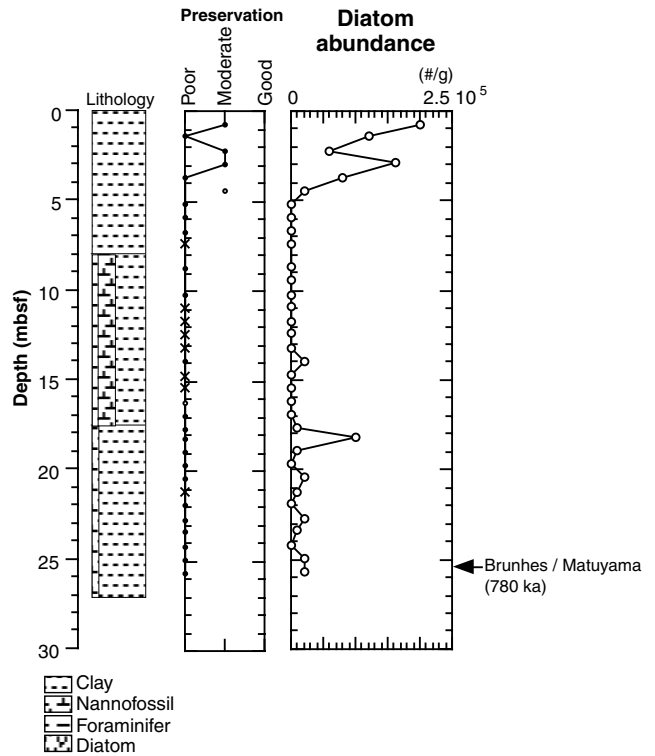


Figure 4. Stratigraphic variations in the abundance and preservation of diatom valves in Hole 1021B. The Brunhes/Matuyama paleomagnetic boundary was derived from Shipboard Scientific Party (1997).

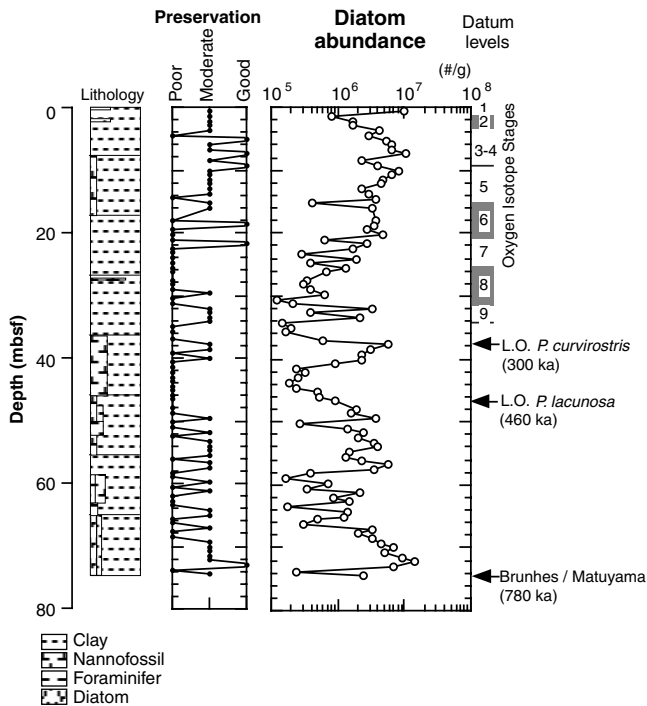


Figure 3. Stratigraphic variations in the abundance and preservation of diatom valves in Hole 1020B. Oxygen isotope stages were derived by A. Mix (pers. comm., 1998). LO (last occurrence) of *Proboscia curvirostris* was from Table 2 (this chapter), and other datum levels were from Shipboard Scientific Party (1997).

REFERENCES

Baldauf, J.G., and Iwai, M., 1995. Neogene diatom biostratigraphy for the eastern equatorial Pacific Ocean, Leg 138. In Pisias, N.G., Mayer, L.A., Janecek, T.R., Palmer-Julson, A., and van Andel, T.H. (Eds.), *Proc. ODP, Sci. Results*, 138: College Station, TX (Ocean Drilling Program), 105–128.

Cande, S.C., and Kent, D.V., 1995. Revised calibration of the geomagnetic polarity timescale for the Late Cretaceous and Cenozoic. *J. Geophys. Res.*, 100:6093–6095.

Ikeda, A., Okada, H., and Koizumi, I., 2000. Data report: late Miocene to Pleistocene diatom from the Blake Ridge Site 997. In Paull, C.K., Matsumoto, R., Wallace, P.J., and Dillon, W.P. (Eds.), *Proc. ODP, Sci. Results*, 164: College Station, TX (Ocean Drilling Program).

Jansen, J.H.F., Kuijpers, A., and Troelstra, S.R., 1986. A mid-Brunhes climatic event: long-term changes in global atmospheric and ocean circulation. *Science*, 232:619–622.

Koizumi, I., 1992. Diatom biostratigraphy of the Japan Sea: Leg 127. In Pisiotto, K.A., Ingle, J.C., Jr., von Breyman, M.T., Barron, J., et al., *Proc. ODP, Sci. Results*, 127/128 (Pt. 1): College Station, TX (Ocean Drilling Program), 249–289.

Shipboard Scientific Party, 1997. Leg 167 introduction. In Lyle, M., Koizumi, I., Richter, C., et al., *Proc. ODP, Init. Repts.*, 167: College Station, TX (Ocean Drilling Program), 5–13.

Yanagisawa, Y., and Akiba, F., 1998. Refined Neogene diatom biostratigraphy for the northwest Pacific around Japan, with an introduction of code numbers for selected diatom biohorizons. *J. Geol. Soc. Jpn.*, 104:395–414.

Date of initial receipt: 19 October 1998

Date of acceptance: 25 August 1999

Ms 167SR-231

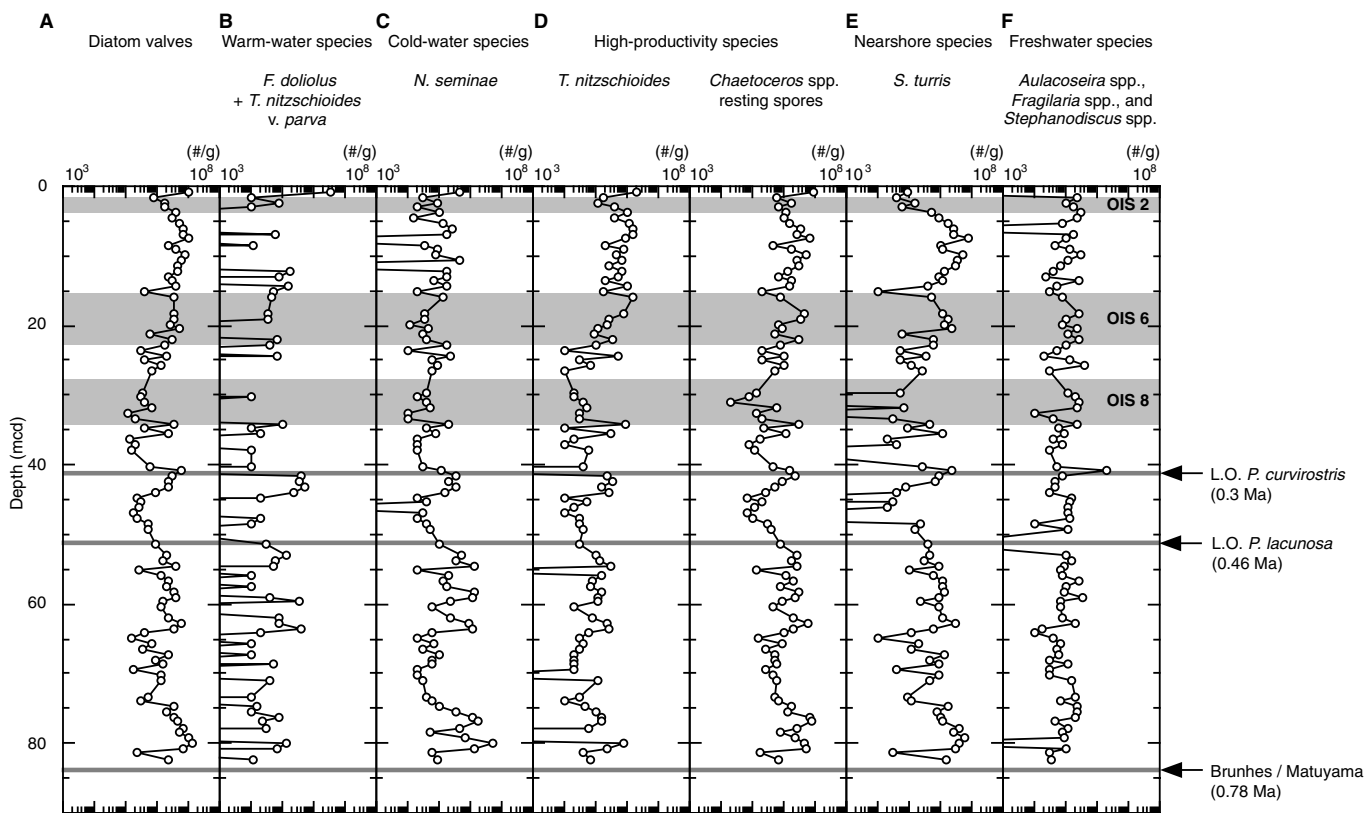


Figure 5. Time series of (A) diatom valves, (B) warm-water species *Fragilariopsis doliolus* and *Thalassionema nitzschioides* var. *parva*, (C) cold-water species *Neodenticula seminae*, (D) high-productivity species *Thalassionema nitzschioides* and *Chaetoceros* spp. (resting spores), (E) nearshore species *Stephanopyxis turris*, and (F) freshwater species *Aulacoseira* spp., *Fragilaria* spp., and *Stephanodiscus* spp. at Site 1020. Shaded areas show glacial periods according to A. Mix (pers. comm., 1998), and shaded lines depict datum levels. LO = last occurrence, OIS = oxygen isotope stage.

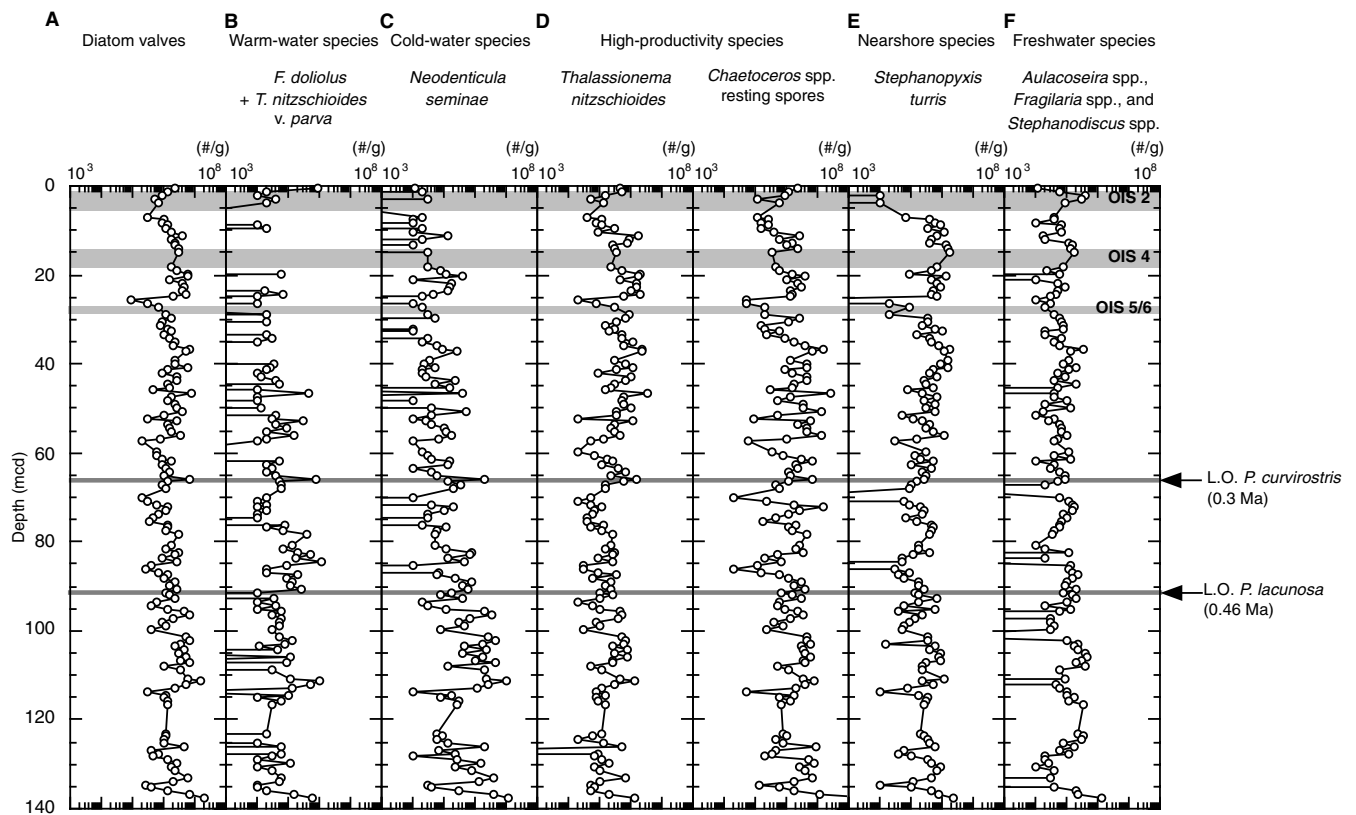


Figure 6. Time series of (A) diatom valves, (B) warm-water species *Fragilariopsis doliolus* and *Thalassionema nitzschioides* var. *parva*, (C) cold-water species *Neodenticula seminae*, (D) high-productivity species *Thalassionema nitzschioides* and *Chaetoceros* spp. (resting spores), (E) nearshore species *Stephanopyxis turris*, and (F) freshwater species *Aulacoseira* spp., *Fragilaria* spp., and *Stephanodiscus* spp. at Site 1018. Shaded areas show glacial periods according to Andreasen (Chap. 8, this volume), and shaded lines depict datum levels. LO = last occurrence, OIS = oxygen isotope stage.

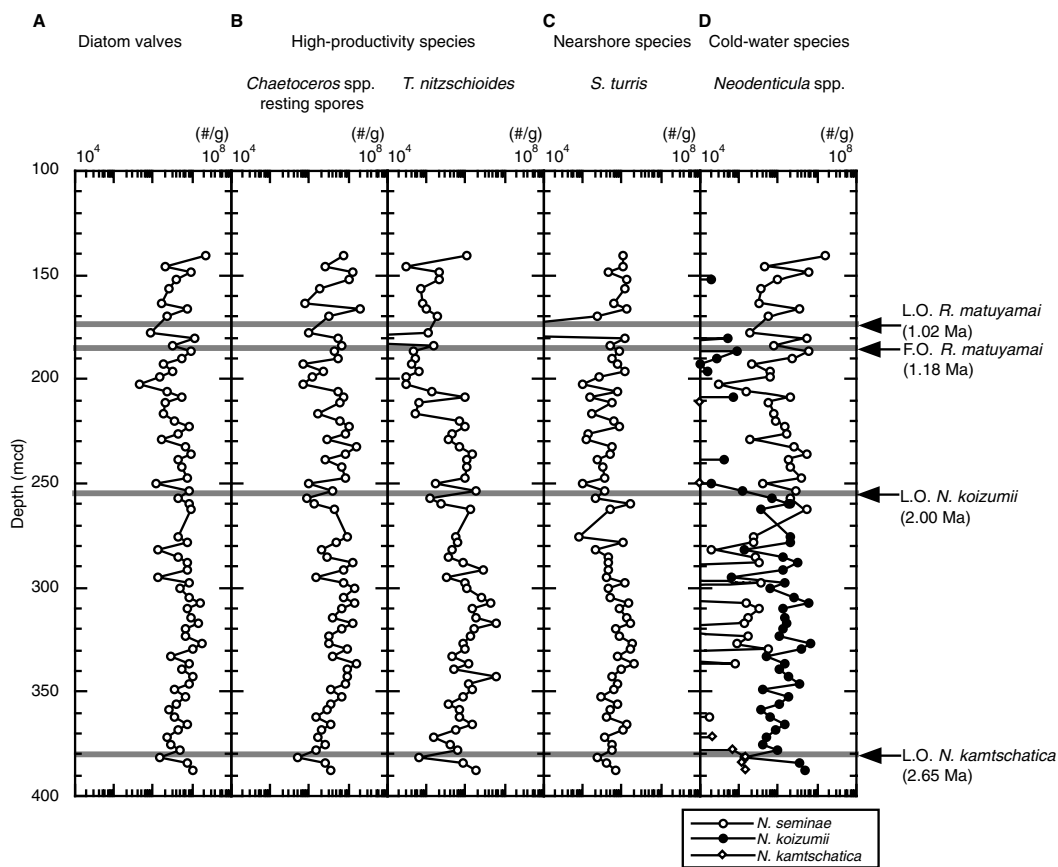


Figure 7. Time series of (A) diatom valves, (B) high-productivity species *Chaetoceros* spp. (resting spores) and *Thalassionema nitzschioides*, (C) nearshore species *Stephanopyxis turris*, and (D) cold-water species *Neodenticula* spp. (*N. kamschatica*, *N. koizumii*, and *N. seminae*) at Site 1018. Shaded lines show datum levels recognized in this work. LO = last occurrence, FO = first occurrence.